Ab initio diffusional potential energy surface for CO chemisorption on Pd{110} at high coverage: Coupled translation and rotation

P. Hu
Department of Chemistry, University of Cambridge, Lensfield Rd., Cambridge, CB2 1EW, United Kingdom, and School of Chemistry, The Queen's University of Belfast, Belfast BT9 5AG, United Kingdom

D. A. King
Department of Chemistry, University of Cambridge, Lensfield Rd., Cambridge, CB2 1EW, United Kingdom

S. Crampin,[a] M.-H. Lee,[b] and M. C. Payne
Cavendish Laboratory, University of Cambridge, Cambridge CB3 0HE, United Kingdom

(Received 17 April 1997; accepted 12 August 1997)

The ground state potential energy surface for CO chemisorption across Pd{110} has been calculated using density functional theory with gradient corrections at monolayer coverage. The most stable site corresponds well with the experimental adsorption heat, and it is found that the strength of binding to sites is in the following order: pseudo-short-bridge>atop>long-bridge>hollow. Pathways and transition states for CO surface diffusion, involving a correlation between translation and orientation, are proposed and discussed. © *1997 American Institute of Physics.* [S0021-9606(97)01743-1]

I. INTRODUCTION

Potential energy surfaces for molecular chemisorption on metal surfaces provide a basis for understanding interactions between molecule and surface. In particular, direct information can be derived for chemisorption energies, surface diffusion activation energy barriers, and diffusion mechanisms. In this paper, we show the potential energy surface (PES) for molecular chemisorption on a solid surface, derived *ab initio* from density functional theory with gradient corrections. We also display the detailed variable orientation of chemisorbed molecules undergoing frustrated translation. The physical origin of this frustrated translation motion is discussed.

CO/Pd{110} was chosen for this study, which was essentially motivated by two factors.

(i) CO chemisorption on Pd{110} is currently a subject of controversy, despite the extensive literature on CO adsorption.[1,2] On this surface, CO exists in three phases, as follows.[3,4] Up to a fractional coverage of about 0.3, CO molecules are adsorbed in a disordered fashion on the unreconstructed Pd{110} surface, producing a (1×1) low energy electron diffraction (LEED) pattern with a high background intensity. In the range $0.3<\theta<0.75$, CO adsorption induces a missing row reconstruction of the Pd{110} surface,[4] but when the coverage is raised to one monolayer the reconstruction is lifted to give a (2×1) $p1g1$ phase. From a detailed infrared spectroscopy study over a wide temperature range, Raval *et al.*[3] concluded that CO molecules adsorb preferentially on short-bridge sites at monolayer coverage. Later, a LEED I–V spectra analysis[5] showed that the agreement between calculated LEED I–V spectra from CO on short-bridge sites with experimental data is worse than calculated spectra from CO on atop sites, in contrast with the infrared results. From a subsequent photoelectron diffraction analysis, based on a relatively small database, it was concluded that the short-bridge site is correct,[6] conflicting with the LEED analysis. Obviously, further studies are called for.

(ii) The process of the surface diffusion of molecules on a solid surface is important. It is often the controlling step in many surface processes, such as surface reactions and epitaxial growth. For example, in the Langmuir–Hinshelwood mechanism, which is the most common catalytic surface reaction mechanism, the surface diffusion of adsorbed molecules is an important elementary step. Taking CO oxidation as an example, the basic reaction mechanism is the Langmuir–Hinshelwood,[7] involving the diffusion of CO as an essential elementary step, since O adatoms are strongly bonded and hence less mobile. A study of CO surface diffusion is therefore an important first step in tackling CO oxidation reactions.

The vibrational mode leading to the diffusion of adsorbed molecules is the frustrated translation. The frequencies of these modes are usually low and close to substrate vibrational frequencies. Thus, a strong coupling between these modes and substrate modes is to be expected, and they are readily excited upon thermal excitation. Despite its importance, little is known about the subject.

The frustrated translational mode of adsorbed molecules on solid surfaces has been observed by several techniques. Several systems, CO/Ru{100},[8] CO/Cu{100},[8] and NO/Ni{111},[9] were studied indirectly through detailed temperature-dependent line shape analyses of high-lying vi-

[a]Present address: School of Physics, University of Bath, Bath, BA2 7AY, United Kingdom.
[b]Present address: Department of Physics, Tamkang University, Taiwan.

brational modes, while others, CO/Pt{111},[10] CO/Ni{100},[11] and CO/Ni{111},[12] have been directly measured by He atom scattering and inelastic electron scattering. Other techniques such as electron stimulated desorption ion angular distribution,[13,14] photoelectron diffraction,[15] and low energy electron diffraction (LEED)[16] have also been used to study the frustrated translational motion of adsorbed molecules. On the other hand, theoretical studies are rare. It would be of importance to study these prediffusive motions theoretically. Finally, anisotropic molecular surface diffusion has recently been reported for CO on Ni{110},[17–19] and it would clearly be of interest to determine the PES relevant to such diffusional motion.

This paper is organized as follows. In the next section, we describe the methodology of our calculations with some test results for the CO molecule, bulk Pd, and a CO–Pd cluster. In the first part of the third section, a potential energy surface from *ab initio* calculations for CO chemisorption on Pd{110} is presented, which supports the conclusion of the infrared study that CO molecules adsorb on pseudo-short-bridge sites at monolayer coverage. In the second part, the time-dependent configuration of chemisorbed CO undergoing frustrated translation is shown. By displaying some molecular-orbital-derived Bloch states, we aim to provide insight into the understanding of the frustrated translation.

II. METHODOLOGY

Ab initio total energy calculations within the density functional theory (DFT) framework were carried out in this study. A type of Car–Parrinello[20] approach, the conjugate gradients minimization scheme, was utilized to directly locate electronic ground states, thus speeding up the calculation considerably compared to the traditional scheme for large systems.[21] The basis set consists of plane waves. The supercell approach was employed to model periodic geometries. A Fermi smearing of 0.5 eV was utilized and the corrected energy extrapolated to zero temperature by the method of Gillan and De Vita,[22,23] which reduces considerably k-point sampling. Both local density approximation (LDA) and gradient corrections were used in our calculations.

Ab initio nonlocal pseudopotentials of C, O, and Pd in fully separable Kleinman–Blylander form were generated by using a kinetic-energy-filter optimization scheme,[24–26] in which electrons of $2s$ and $2p$ in C, $2s$ and $2p$ in O, and $4d$, $5s$, and $5p$ of Pd were treated as valence electrons and the rest of the electrons were included in core potentials. It was found that a 500 eV cutoff energy was high enough to obtain properties we are interested in. A $p(2\times1)$ unit cell was used in our calculations, which corresponds to 5.50×3.89 Å^2 in the surface plane. Pd{110} was modeled using a supercell with three Pd layers and a vacuum layer thicker than 8 Å. The sampling of the k-grid was $4\times5\times1$.

In recent studies, it was found[27,28] that LDA calculations yield chemisorption energies which are significantly higher than experimental values but the inclusion of gradient corrections gives better agreement. It was also found[27] that sites for CO chemisorption with higher coordination of the adsorbate to surface atoms lead to a larger degree of overbinding with LDA, and give larger corrections with gradient corrections. In this study, the generalized gradient approximation (GGA) of Perdew and Wang[29] was used, while the Ceperly–Alder exchange-correlation energy was employed in LDA calculations.

TABLE I. A comparison between calculated and experimental properties of free CO. LDA is the local density approximation and GGA is the generalized gradient approximation.

	Exp.	LDA	GGA
C–O bond length (Å)	1.1283	1.1281	1.1257
Error in bond length		−0.02%	−0.23%
Vibrational frequency (cm^{-1})	2143	2167	2206
Error in vibrational frequency		1.1%	2.9%

Some physical and chemical properties of the CO molecule, bulk Pd, and CO on a Pd cluster were tested. In the CO molecule calculations, the molecule was placed in a box. Table I lists LDA and GGA calculation results for CO bond length and vibrational frequency, which were obtained self consistently. It is clear that there is good agreement with experimental bond length and vibrational frequency from both LDA and GGA. Table II shows some calculated bulk properties of Pd. A CO–Pd cluster was chosen, in which a linear O–C–Pd was placed in a box. Some results are listed in Table III. Although there is no direct experimental data, C–Pd and C–O bond lengths are reasonable compared to available experimental values from analogous compounds.[30,31] From Table I to III, we can see clearly that LDA in our calculations produces good geometric structures and vibrational frequencies, while there is no improvement using GGA. On the other hand, the overbinding is very obvious from LDA calculations, and GGA produces much better bonding energies compared to experimental work (Table III).

III. RESULTS AND DISCUSSIONS

A. Potential energy surface of CO/Pd{110}

To generate the potential energy surface for CO chemisorption on Pd{110}, schematically shown in Fig. 1, we computed two slices, one along AB and the other along CD, by moving the carbon atom positions along these directions. Total energies are obtained by fixing the C atom positions in the surface plane but allowing relaxation along the surface normal; O atoms were allowed to move in any direction to lower the energy, according to forces calculated by the Hellmann–

TABLE II. A comparison between calculated and experimental bulk lattice constants of Pd.

	Experiment	LDA	GGA
Lattice constant (Å)	3.89	3.94	4.03

TABLE III. A comparison between calculated and experimental (Refs. 30 and 31) properties of Pd–CO. The overbinding of LDA can be clearly seen.

	LDA	GGA	Exp.
Pd–C bond length (Å)	1.90	1.92	1.93[a]
C–O bond length (Å)	1.14	1.14	1.15[a]
Bonding energy of Pd–CO (eV)	2.47	1.72	1.6[b]

[a]From CO/Pd{100}, Ref. 30.
[b]From CO/Pd{100}, Ref. 31.

Feynman theorem and total energies. All the results shown in this paper were obtained by using the symmetry of the unit cell to save computing time. Consequently, the forces along ⟨110⟩ are zero. However, we also did some calculations without imposing any symmetry, and found that the forces on CO were negligible along ⟨110⟩ compared to the forces along ⟨001⟩. Chemisorption energies are calculated by subtracting the total energy of CO/Pd{110} from the total energy of the CO molecule and Pd substrate. It is clear from Fig. 2(a) that the pseudo-short-bridge site in which C atoms are laterally displaced by about 0.6 Å from the symmetric short-bridge site gives rise to the strongest bonding (-1.43 eV, in very good agreement with the experimental value of -1.55 eV[3]), while the hollow site leads to the weakest bonding. The short-bridge site is about 0.3 eV more stable than the top site. The stability of the pseudo-short-bridge site rather than the symmetric short-bridge site is due to CO–CO repulsion, along the close packed rows, which is reduced by alternately tilting CO molecules sitting on adjacent Pd atoms away from each other. We expect that CO would adsorb on short-bridge sites at lower coverages. This result supports the infrared

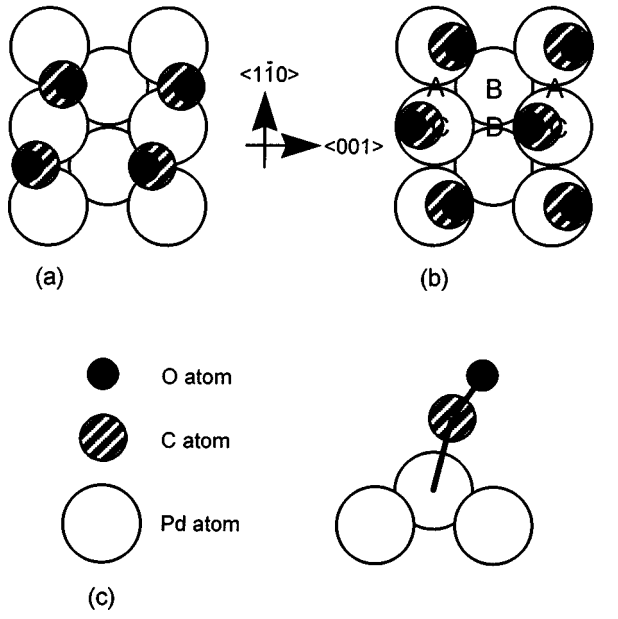

FIG. 1. Schematic illustrations of (a), (b) an fcc {110} surface and (c) the CO tilt angle.

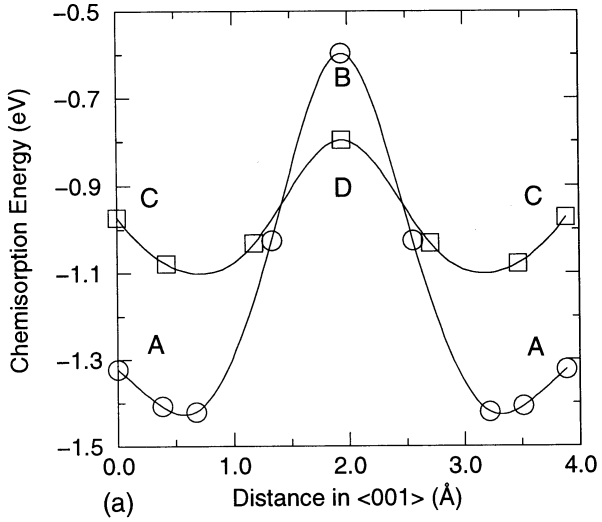

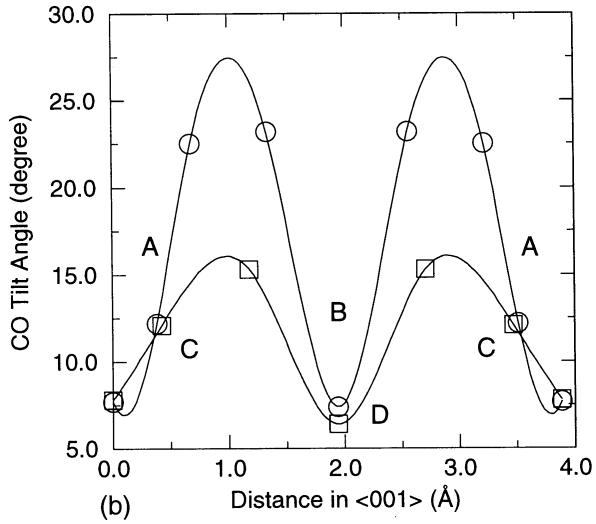

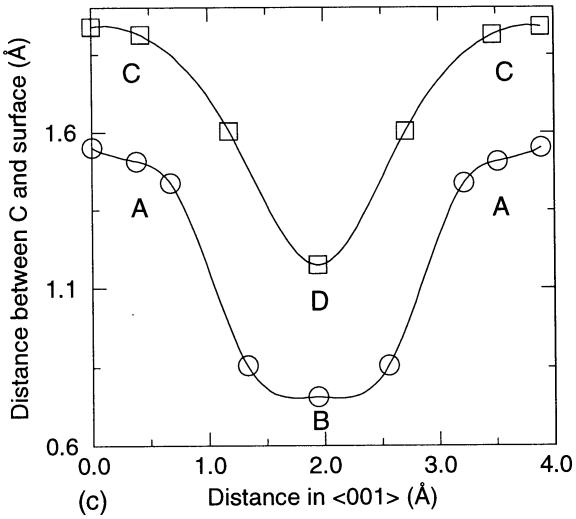

FIG. 2. (a) Computed ground state chemisorption energies for CO on Pd{110}, along ⟨001⟩ in the two directions *ABA* and *CDC* defined in Fig. 1. The most favorable site is displaced 0.6 Å along ⟨001⟩ from the short-bridge site *A*, and the least favorable is the hollow site *B*. (b) The CO tilt angles along *ABA* and *CDC*. (c) The vertical displacement of the CO C atom, relative to top-layer Pd atom centers, along *ABA* and *CDC*.

assignment.[3] A recent photoelectron diffraction study[6] favored the short-bridge site. The present work therefore supports this assignment, but not that of a LEED study.[5]

From the data presented in Fig. 2(a), the PES for CO diffusion on Pd{110} has been constructed, as shown in Fig. 3. A polynomial interpolation procedure was used to generate this figure, based on the two slices shown in Fig. 2(a). Some years ago Doyen and Ertl[32] calculated diffusional potential energy surfaces for CO on Cu, Ni, and Pd surfaces using the Anderson–Grimley–Newns formalism, with results that have not been borne out by experiment. Our potential energy surface shown in Fig. 3 is qualitatively and quantitatively different from their results. The failure of the application of the Anderson–Grimley–Newns formalism in calculating potential energy surfaces is not surprising, given the small energy differences between different chemisorption sites. To obtain an accurate potential energy surface is very demanding, and any major approximation can lead to misleading results. For example, we have shown, as mentioned above, that with LDA the degree of overbinding depends on site coordination,[27] and this would dramatically alter the diffusional PES.

Using optical diffraction from a laser-induced monolayer grating, Shen and co-workers[17–19] recently made the first measurements of the anisotropic diffusion of CO on Ni{110}. In the coverage range up to ~0.7 monolayer, diffusion activation energies of 0.17 and 0.20 eV along ⟨110⟩ and ⟨001⟩, respectively, were reported. They proposed diffusion pathways for CO on Ni{110} from short to short-bridge sites via top sites along ⟨110⟩ and from short bridge to short-bridge sites via hollow sites along ⟨001⟩, as shown in Fig. 4(a). The proposed transition states for diffusion are marked with crosses in the figure. We now propose alternative pathways for CO on Pd{110} based on our calculated potential energy surface. As shown in Fig. 3, along ⟨110⟩, CO simply diffuses from short bridge to short-bridge sites through top sites, as suggested by Shen and co-workers.[17] The diffusion activation energy barrier is about 0.3 eV at low temperatures. Along ⟨001⟩, however, it is likely that the minimum energy pathway avoids the hollow site, passing instead through a saddle point at *D*. This pathway is also shown in Fig. 4(b). In the transition state, CO is bonded in the long bridge site to two Pd atoms in the top layer. The diffusion activation energy barrier along this direction is about 0.6 eV at low temperatures. Of course, it must be stressed that the above discussions are based on calculations with monolayer CO. With vacancies, the potential energy surface may be different, particularly for CO diffusion at low coverages. However, we found that there is no direct bonding between CO molecules, and the CO–metal bonds are relatively strong at monolayer coverage. In other words, CO–CO interactions are much weaker than CO–metal interactions. We therefore expect that the potential energy surface shown in Fig. 3 is mainly determined by the interaction between CO and Pd, and the key features discussed above will even apply to CO diffusion at quite low coverages.

The striking feature in this potential energy surface is the large barrier at the hollow site. This may be understood as

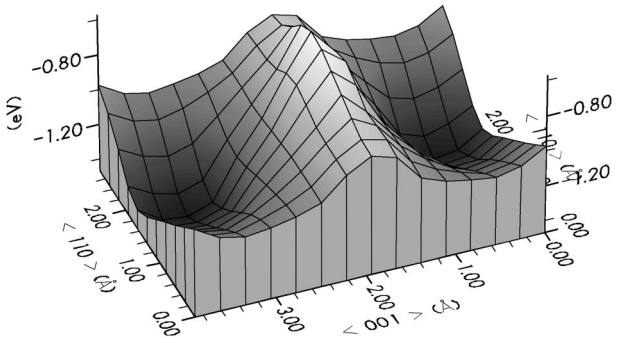

FIG. 3. The computed potential energy surface for the surface diffusion of CO on Pd{110} constructed from Fig. 2(a), plotted as a function of the C atom positions across the surface unit mesh, corresponding to monolayer coverage.

follows. At this site, CO is bonded atop to a second layer Pd which is less stable than the bridge site. More importantly, the high charge density generated at this site by *sp* electrons on neighboring top layer Pd atoms prevents the CO molecule from approaching sufficiently close to the second layer atom to form an optimal overlap with the tightly bound *d* states which provide most of the bonding.[33] The neighboring hollow site, the long bridge, provides more optimal bridge bonding, but again the overlap between CO molecular orbitals and metal *d* orbitals on this site is poor.

B. Physical origin of frustrated translation

In Fig. 2(b), we show optimal CO tilt angles for CO surface diffusion from short bridge to hollow and to short-bridge sites displaying in curve *ABA*, and from top to long bridge and to top sites showing in curve *CDC*. In both cases, the optimal CO tilt angle shows a strong variation as the molecule is moved across the unit cell, with small tilt angles (~7°) at the symmetric short bridge or atop sites, and at the hollow and long-bridge sites, and large tilt angles (~27° along *AB* and ~16° along *CD*) at intermediate locations. This may not seem immediately obvious: why the CO tilt angle increases and then decreases as the molecule moves

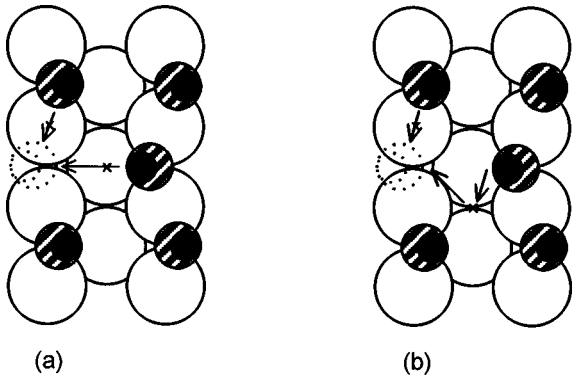

FIG. 4. Proposed CO surface anisotropic diffusion pathways on {110} surfaces. (a) The surface diffusion pathways proposed by Shen and co-workers (Ref. 17) for CO on Ni{110}, where the crosses mark the transition states. (b) The surface diffusion pathways we propose for CO on Pd{110}, based on the PES in Fig. 3.

from short bridge to hollow sites. The same is true from top to long-bridge sites. In this section, we address the physical origin of these striking CO axial variations.

In our *ab initio* total energy calculations, total charge densities are obtained as

$$\rho_{\text{total}}(\mathbf{r}) = \sum_{i_{\text{band}}} \sum_{\mathbf{k}_j} \rho_{i_{\text{band}},\mathbf{k}_j}(\mathbf{r}) = \sum_{i_{\text{band}}} \sum_{\mathbf{k}_j} |\psi_{i_{\text{band}},\mathbf{k}_j}(\mathbf{r})|^2,$$

where i_{band} is a band number; $\mathbf{k}_j$ is a $\mathbf{k}$-point; the first and second summations run over all occupied bands and sampled $\mathbf{k}$-points, respectively; and $\psi_{i_{\text{band}},\mathbf{k}_j}$ is a well-defined Bloch state. In a recent study, we examined the charge densities of individual Bloch states, $\rho_{i_{\text{band}},\mathbf{k}_j}$, in real space for a CO chemisorption system[33]; this approach provides strikingly clear insight into the bonding between molecules and extended surfaces.[33] Most bonding comes from the mixing of the CO 5σ orbital with Pd *d* states, forming some antibonding states above the Fermi level, and Pd *d* states with the CO 2π state, forming bonding states below the Fermi level. Here we use this approach again to examine the nature of the chemical bond as the molecule is moved across the unit cell, in order to understand the CO tilt angle variations.

In Figs. 5 and 6, we display 2D cuts of the CO 5σ-orbital derived Bloch states in real space for C atom positions of CO at 0.0 [short-bridge site, Figs. 5(a) and 6(a)], 0.38 (b), 0.67 (c), 1.33 (d), and 1.95 Å (hollow site, *e*) from the short-bridge site, respectively. The cuts in Fig. 5 are parallel to ⟨001⟩ and through O, C, and two Pd atoms in the *second* layer, which are shown as *ABCD* in Fig. 7(a), while the cuts in Fig. 6 are perpendicular to ⟨001⟩ and through O and C atoms, which are shown as *EFGH* in Fig. 7(b), and pass through Pd atoms in the top layer. Any bonding between CO and *top*-layer atoms should show up as *d* character in Figs. 6(a) to 6(e), while bonding to second-layer atoms in the troughs between the top-layer rows should show up as *d* mixing in Figs. 5(a) to 5(e). From Figs. 5 and 6, it is clear that CO bonds to the short-bridge site along top-layer rows [Figs. 6(a) and 6(b)], and there is no bonding between CO and Pd atoms in the second layer [Figs. 5(a) and 5(b)] when the C atom of CO is 0.0 and 0.38 Å away from the short-bridge site, which is not surprising. It can be seen in Figs. 5(c) and 6(c) that CO still bonds to the short-bridge site rather than the pseudo-3-fold site when the C atom of CO is 0.67 Å away from the short-bridge site. At the hollow site, the bonding has been switched from CO to the single second Pd layer atom, as clearly shown in Fig. 5(e); there is also now clearly no bonding to top-layer atoms, as shown in Fig. 6(e). Obviously, on both the symmetric short bridge and hollow sites, the ideal configuration of the CO axis is upright. Since there is a repulsion between CO molecules at monolayer coverage, the CO molecules do tilt away from each other, leading to small tilt angles at these sites. When the C atom is 1.33 Å away from the short-bridge site, CO bonds to both the top-layer short-bridge site, shown in Fig. 6(d), and the second Pd layer atom, shown in Fig. 5(d).

We therefore find that the CO axis angular variations can be attributed to the changing nature of the chemical bond as

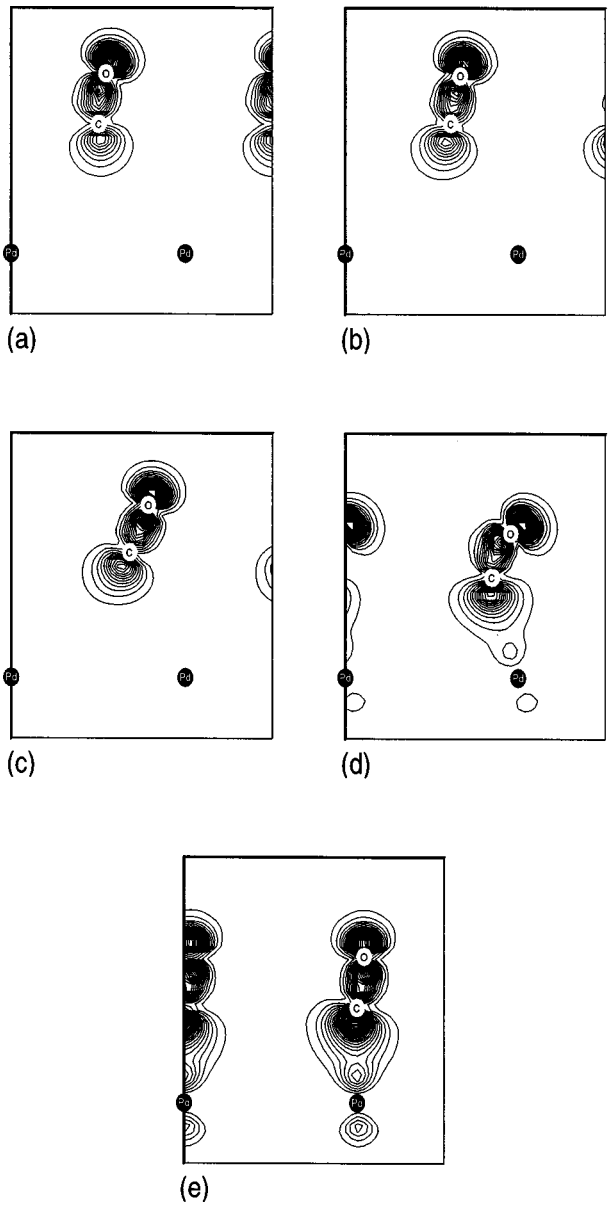

FIG. 5. Illustration of bonding between CO and Pd{110} for several different CO positions from short-bridge to hollow sites using CO 5σ-derived states. (a), (b), (c), (d), and (e) are 2D contours of charge densities of CO 5σ-derived Bloch states (Ref. 33) for CO at 0.0, 0.38, 0.67, 1.33, and 1.95 Å from the short-bridge site respectively, cutting through the O, C, and two Pd atoms in the second layer, shown as *ABCD* plane in Fig. 7(a).

the molecule is moved across the unit cell. Taking the displacement along *AB*, CO is initially bridge-bonded to two top-layer Pd atoms. At the midpoint between site A, the short bridge, and site B, the hollow site, where the C atom is 1.33 Å away from the short-bridge site, the CO molecule is still essentially bridge-bonded to the same two top-layer Pd atoms, although some charge density is beginning to accumulate between the C atom and a second-layer Pd atom. The effort to maintain this bridge-bonding configuration results in the large tilt angle at this point [Fig. 2(b)]. Further movement produces (unfavorable) bonding to the second-layer Pd atom, and the CO axis moves back toward the upright position. As a consequence, the translational motion of the molecule

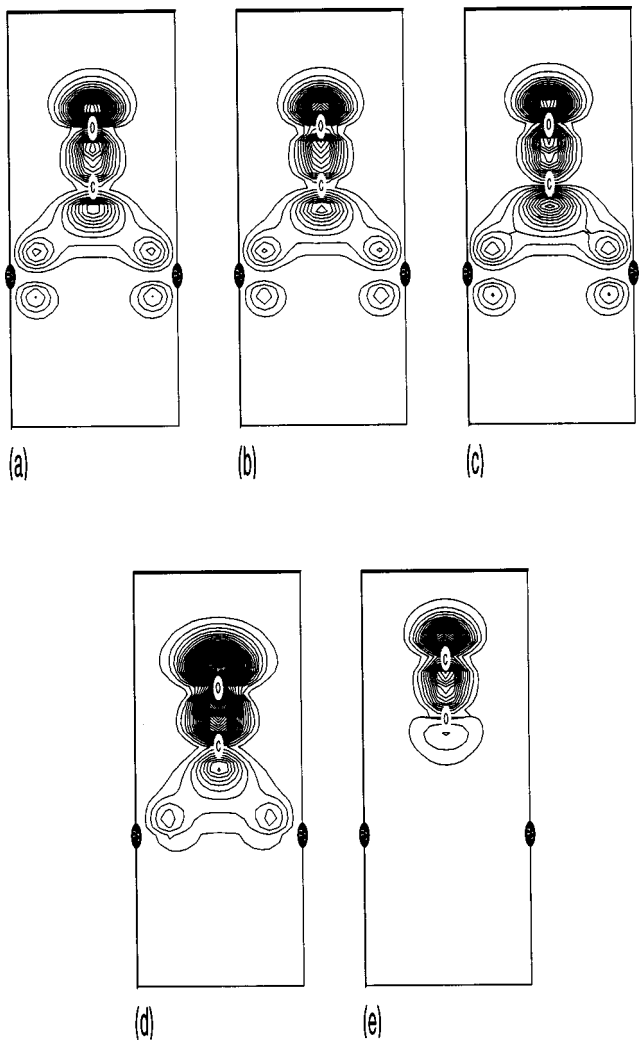

FIG. 6. Illustration of bonding between CO and Pd{110} for several different CO positions from short-bridge to hollow sites. (a), (b), (c), (d), and (e) are 2D contours of charge densities of CO 5σ-derived Bloch states corresponding to (a), (b), (c), (d), and (e) in Fig. 5, respectively, cutting through the O, C, and two Pd atoms in the first layer, shown as *EFDH* in Fig. 7(b).

across *ABA* is coupled to a hindered rotational motion of the molecule. As shown in Fig. 2(c), this motion is also accompanied by a relatively large corrugation, of ~ 0.8 Å, as the C atom sinks into the hollow site B or the long-bridge site D. It was anticipated that the translation of molecules across surfaces would be coupled to a hindered rotational motion. Perez Jigato, Walter, and King[34] performed a liquid helium temperature NEXAFS study on NO/Pd {110} and determined the temperature dependence of the π^* and the σ^* resonance cross sections. Their results showed strongly anharmonic behavior, and it was suggested[34] that translational motion was accompanied by a change in tilt angle. The present results provide quantitative support for this conclusion. We note that the tilt angles along *AB* are larger than that along *CD*, which is probably due to differences in the corrugation wells at *B* and *D*.

IV. CONCLUSIONS

In summary, we have calculated the diffusional ground state potential energy surface for CO chemisorption on Pd{110}, shown in Fig. 3, within the density functional theory framework with gradient corrections. The potential energy surface is both qualitatively and quantitatively different from previous potential energy surfaces obtained using the Anderson–Grimly–Newns formalism. We find that the most stable site, with an adsorption heat of -1.43 eV (close to the experimental value of -1.55 eV) is the pseudo-short-bridge, and least stable is the hollow site in the trough between top-layer rows. We have also demonstrated a strong correlation between translation and orientation for CO diffusion along ⟨001⟩ and attributed it to the changing nature of the chemical bond during CO diffusion. Along ⟨110⟩, CO diffuses from pseudo-short-bridge to pseudo-short-bridge sites via an on-top site; this being the saddle point, with a barrier of 0.3 eV. Along ⟨001⟩, the diffusion path avoids the

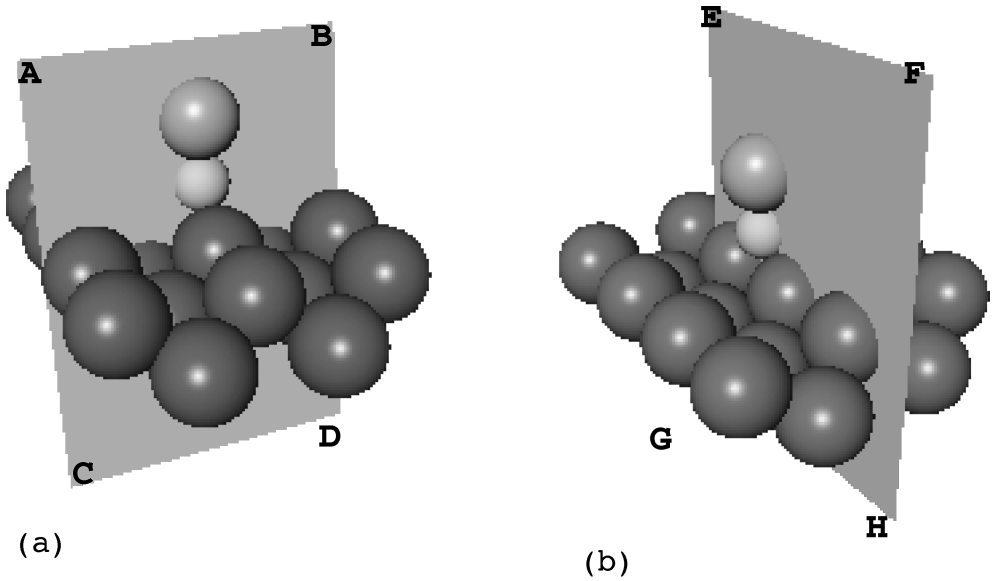

FIG. 7. Schematic illustration of cuts shown in Fig. 5 for CO/Pd{110}. *ABCD* in (a) is parallel to ⟨001⟩ and through O, C, and two Pd atoms in the second layer. *EFGH* in (b) is perpendicular to ⟨001⟩ and through O, C, and two Pd atoms in the first layer.

hollow site, moving across a saddle point at the long-bridge site, with a barrier of 0.6 eV. The switch in bonding as the molecule is moved across the trough from bridged with top-layer atoms to atop with a second-layer Pd atom is clearly demonstrated in charge-density plots of the eigenstates corresponding to the bonding mixed $5\sigma-d$ state formed between CO and metal. It is this switch which is responsible for a coupling between translational and rotational motions of the molecule.

ACKNOWLEDGMENTS

Part of these calculations were performed at the parallel processor machine at Daresbury, U.K.. We acknowledge EPSRC for supporting the work.

[1] J. T. Yates, Jr., Surf. Sci. **299/300**, 731 (1994).
[2] J. C. Campuzano, in *The Chemical Physics of Solid Surfaces and Heterogeneous Catalysis*, edited by D. A. King and D. P. Woodruff (Elsevier, New York, 1990), Vol. 3A, p. 389.
[3] R. Raval, S. Haq, M. A. Harrison, G. Blyholder, and D. A. King, Chem. Phys. Lett. **167**, 391 (1990).
[4] P. Hu, L. M. de la Garza, R. Raval, and D. A. King, Surf. Sci. **249**, 1 (1991).
[5] A. Wander, P. Hu, and D. A. King, Chem. Phys. Lett. **201**, 393 (1993).
[6] A. Locatelli, B. Brena, S. Lizzit, G. Comelli, G. Cautero, G. Paolucci, and R. Rosei, Phys. Rev. Lett. **73**, 90 (1994).
[7] G. Ertl, Surf. Sci. **299/300**, 742 (1994).
[8] B. N. J. Persson, F. M. Hoffmann, and R. Ryberg, Phys. Rev. B **34**, 2266 (1986).
[9] W. Erley and B. N. J. Persson, Surf. Sci. **218**, 494 (1989).
[10] A. M. Lahee, J. P. Toennies, and Ch. Woll, Surf. Sci. **177**, 371 (1986).
[11] R. Berndt, J. P. Toennies, and Ch. Woll, J. Electron Spectrosc. Relat. Phenom. **44**, 183 (1987).
[12] J. S. Ha and S. J. Sibener, Surf. Sci. **256**, 281 (1991).
[13] M. Kiskinova, A. Szabo, A.-M. Lanzillotto, and J. T. Yates, Jr., Surf. Sci. **202**, L559 (1988).
[14] M. A. Henderson, A. Szabo, and J. T. Yates, Jr., J. Chem. Phys. **91**, 7255 (1989).
[15] V. Fritzsche, K.-M. Schindler, P. Gardner, A. M. Bradshow, M. C. Asensio, and D. P. Woodruff, Surf. Sci. **269/270**, 35 (1992).
[16] H. Over, W. Moritz, and G. Ertl, Phys. Rev. Lett. **70**, 315 (1993).
[17] X. D. Xiao, Y. L. Xie, and Y. R. Shen, Phys. Rev. B **48**, 17452 (1993).
[18] X. D. Xiao, X. D. Zhu, W. Daum, and Y. R. Shen, Phys. Rev. B **46**, 9732 (1992).
[19] X. D. Xiao, X. D. Zhu, W. Daum, and Y. R. Shen, Phys. Rev. Lett. **66**, 2352 (1991).
[20] R. Car and M. Parrinello, Phys. Rev. Lett. **55**, 2471 (1985).
[21] M. C. Payne, M. P. Teter, D. C. Allen, T. A. Arias, and J. D. Joannopoulos, Rev. Mod. Phys. **64**, 1045 (1992), and reference therein.
[22] M. J. Gillan, J. Phys.: Condens. Matter **1**, 689 (1989).
[23] A. De Vita and M. J. Gillan, J. Phys.: Condens. Matter **3**, 6225 (1991).
[24] M.-H. Lee, J.-S. Lin, M. C. Payne, V. Heine, V. Milman, and S. Crampin (in preparation).
[25] J.-S. Lin, A. Qteish, M. C. Payne, and V. Heine, Phys. Rev. B **47**, 4174 (1993).
[26] A. Rappe, K. Rabe, E. Kaxiras, and J. D. Joannopoulos, Phys. Rev. B **41**, 1227 (1990).
[27] P. Hu, D. A. King, S. Crampin, M.-H. Lee, and M. C. Payne, Chem. Phys. Lett. **230**, 501 (1994).
[28] P. H. T. Philipsen, G. te Velde, and E. J. Baerends, Chem. Phys. Lett. **226**, 583 (1994).
[29] J. P. Perdew, in *Electronic Structure of Solids*, edited by P. Ziesche and H. Eschrig (Akademie Verlag, Berlin, 1991); J. P. Perdew and Y. Wang (unpublished).
[30] R. J. Behm, K. Christmann, G. Ertl, and M. A. Van Hove, J. Chem. Phys. **73**, 2984 (1980).
[31] J. C. Tracy and P. W. Palmberg, J. Chem. Phys. **51**, 4852 (1969).
[32] G. Doyen and G. Ertl, Surf. Sci. **43**, 197 (1974).
[33] P. Hu, D. A. King, M.-H. Lee, and M. C. Payne, Chem. Phys. Lett. **246**, 73 (1995).
[34] M. Perez Jigato, W. K. Walter, and D. A. King, Surf. Sci. **301**, 273 (1994).